JCTC Journal of Chemical Theory and Computation

Article

pubs.acs.org/JCTC

The Solvation Structure of Na^+ and K^+ in Liquid Water Determined from High Level *ab Initio* Molecular Dynamics Simulations

Christopher N. Rowley and Benoît Roux*

Department of Biochemistry and Molecular Biology, The University of Chicago, 929 East 57th Street, Chicago, Illinois, United States

Supporting Information

ABSTRACT: Knowledge of the hydration structure of Na^+ and K^+ in the liquid phase has wide ranging implications in the field of biological chemistry. Despite numerous experimental and computational studies, even basic features such as the coordination number of these alkali ions in liquid water, thought to play a critical role in selectivity, continue to be the subject of intensive debates. Simulations based on accurate potential energy surfaces offer one approach to resolve these issues by providing reliable results on ion hydration. In this article, we report the results from molecular dynamics simulations of Na^+ and K^+ hydration based on a novel and rigorous strategy designed to overcome the challenges of QM/MM simulations of solvent molecules in the liquid phase. In this method, which we call Flexible Inner Region Ensemble Separator (FIRES), the ion and a fixed number of nearest water molecules form a dynamical and flexible inner region that is represented with high level ab initio quantum mechanical (QM) methods, while the water molecules from the surrounding bulk form an outer region that is represented by a polarizable molecular mechanical (MM) force field. Simulations yield rigorously correct thermodynamic averages as long as the solvent molecules in the flexible inner and outer regions are not allowed to exchange. Extensive FIRES simulations were carried out based on a QM/MM model in which the Na^+ or K^+ ion and the 12 nearest water molecules were represented by high level ab initio methods (RI-MP2/def2-TZVP and density functional theory with PBE/def2-TZVP), while the surrounding MM water molecules were represented by the polarizable SWM4-NDP potential. On the basis of these results, the ion coordination numbers are estimated to be within the range of 5.7−5.8 for Na^+ and 6.9−7.0 for K^+.

INTRODUCTION

The solvation of ions by liquid water and their association with biological molecules is a subject of critical importance in biology and biochemistry.[1] In particular, it is believed that subtle differences in the coordination structure of Na^+ and K^+, two of the most prevalent ions, might play a central role in the high selectivity required for the function of membrane channels and transporters. While there have been extensive experimental and computational studies of the hydration of Na^+ and K^+, a definitive picture of how these ions are solvated in water is lacking, and many questions concerning the organization of water molecules in their vicinity remain unresolved.

There have been several attempts to determine $g(r)$, the ion−water radial distribution functions (RDF), which gives the relative density of the solvent at a given distance r from the ion,[2] using X-ray and neutron scattering.[3,4] Ion−solvent RDFs are typically dominated by a maximum at short distance, corresponding to the first coordination shell of solvent molecules. An early neutron diffraction study by Neilson and Skipper[5] concluded that the solvation structure of K^+ was broader and much more disordered in comparison to Li^+. More recently, a neutron diffraction study by Soper and Weckström[6] and an Extended X-ray absorption fine structure (EXAFS) study by Glezakou et al. provided additional quantification of the first peak of the RDF.[7] Na^+ hydration has received less attention, although Skipper and Neilson were able to determine an approximate Na^+−O RDF through X-ray and neutron scattering using Ag^+ as an isomorphic ion.[8] The overlap of M−O correlations with M−H and O−O correlations, in addition to other inherent limitations of this methodology, has prevented a fully conclusive experimental description of Na^+ and K^+ solvation. Despite decades of investigation, there is still dispute about the ion−water RDFs and the average number of water molecules within the first hydration shell of Na^+ and K^+.

Molecular dynamics (MD) simulation is an obvious strategy to deepen our knowledge of ion solvation, although such computational results must be interpreted with caution because the details of ion solvation are sensitive to the underlying molecular mechanical (MM) potential energy surface. Most force field models representing ion−water interactions have been empirically optimized by targeting the enthalpy of the monohydrate and the absolute hydration free energy. Åqvist was one of the first to adopt this strategy to systematically develop a set of Lennard-Jones parameters for the alkali-halide series, adapted to the nonpolarizable SPC water model.[9,10] Lennard-Jones parameters for ions have also been optimized according to a similar strategy for the CHARMM[11] and AMBER[12] force fields, which are parametrized for use with the nonpolarizable TIP3P water model.[13] Generally, the trends displayed from such MD simulations were that Na^+ has a well-ordered first hydration sphere with a deep first minimum, while K^+ has a more diffuse coordination sphere.[14−16] Average coordination numbers, determined by integrating the first peak of the RDF ($n_c = 4\pi\rho \int_0^{R_i} r^2\, g(r)\, dr$), vary considerably among the different models. One possible shortcoming of these early models is that the parameters were optimized to reproduce the

Special Issue: Wilfred F. van Gunsteren Festschrift

Received: February 1, 2012
Published: April 10, 2012

experimental absolute ion hydration free energies. As the latter rely on "extrathermodynamic" assumptions,[17,18] the target values for the cations and the anions are not uniquely determined and can shift relative to one another in opposite directions depending on the different experimental scales. All absolute single ion hydration free energies deduced from experimental results suffer from such a fundamental offset uncertainty, which undermnes their usefulness for validating a model. The next generation polarizable AMEOBA and Drude models circumvented this problem by targeting the total solvation free energy of the neutral salts instead, although it remains unclear if these models have the ability to accurately describe the local hydration structure, as they have not been parametrized to these data. The lack of reliable and near-definitive target data about the hydration structure of Na^+ and K^+ contributes to increasing the difficulties in refining current force field models.

One avenue to gain information about solvation features that are not immediately accessible by experiments and circumvent the possible limitations of empirical force fields is first-principles ab initio molecular dynamics (AIMD) simulations where the entire simulation system is treated with a quantum mechanical (QM) method. In typical AIMD studies of Na^+ and K^+ hydration, a system comprised of a single ion and a small number of water molecules (~25−50) represented with density functional theory (DFT) was simulated using the CPMD or VASP codes.[16,19−23] As a general trend, AIMD simulations have predicted a hydration structure that is more diffuse than force field models, with a shorter and broader first peak of the RDF and lower coordination numbers for both Na^+ and K^+. The time scale afforded by AIMD simulations is typically on the order of tens of picoseconds, which is sufficient to characterize the RDFs and the coordination number of the ion. However, because it is challenging to calculate macroscopic thermodynamic properties using these short trajectories, it has not been possible to systematically validate the accuracy of these methods by comparing with experimental solvation data.[24]

An alternative strategy consists of partitioning the system into an inner region, where the ion and a set of nearby waters are treated with QM, and an outer region, where the rest of the solvent is represented with a less computationally expensive theory (e.g., dielectric continuum or MM).[25−27] One elegant scheme to rigorously partition the problem of ion solvation into two regions is quasi-chemical theory (QCT),[28] whereby the system is exactly separated into a small fixed spherical subvolume comprising one ion and n water molecules and the second region is comprised of the remaining bulk liquid phase. Thermodynamic ion solvation properties are then expressed as a sum over a series of clusters comprising the ion and n water molecules, each treated at the QM level, and each explicitly weighted by the probability $P(n)$ of finding n waters in the inner region. However, as the determination of $P(n)$ is challenging, QCT does not easily lead to an effective QM/MM simulation strategy.[29]

A more direct approach that avoids the necessity of evaluating $P(n)$ is to allow exchange of the water molecules between the QM and MM representations depending on their distance from the ion during QM/MM simulations. Sampling of such a QM/MM system could possibly be carried out via Metropolis Monte Carlo with a sharp separation between the QM and MM regions, but MD simulations would be impractical due to the discontinuity in the potential energy surface. To avoid this problem, a number of schemes have been designed to smoothly switch between the QM and MM representations when a water molecule goes back and forth across the boundary. The ONIOM-XS[30] and the Adaptive Partitioning method[31] have been used to model Li^+ solvation, while the Quantum Mechanical Charge Field (QMCF) method has been applied to Na^+ and K^+ solvation.[26,27] Using the QMCF method, it was possible to simulate a solvated Na^+ and K^+ ion with waters within 3.0 Å and 3.5 Å (respectively) of the ion treated at the Hartree−Fock level surrounded by an outer region of water molecules represented by the BJK-CF2 model; however, the full power of modern models and high performance computing have not been leveraged fully.

In this paper, we present a comparison of the hydration structure of the first coordination sphere of Na^+ and K^+ from MD simulations based on a novel QM/MM partitioning scheme that does not require the use of a switching region. The n water molecules nearest the ion form a dynamical and flexible inner region that is represented with high level ab initio QM methods, while the remaining water molecules from the surroundings form an outer region that is represented by a polarizable MM force field. Simulations yield rigorously correct thermodynamic averages as long as the solvent molecules from the flexible inner and outer regions are not allowed to exchange. In an attempt to obtain a near-definitive picture of Na^+ and K^+ solvation in liquid water, extensive efforts were made to avoid possible sources of error by using a high level ab initio method with a large QM basis set for the inner region and a very accurate polarizable model for the outer region.

THEORY AND METHOD

QM/MM Model of Ion Solvation. Our model for the Drude and QM/MM ion solvation simulations is comprised of a 14 Å sphere of 451 water molecules surrounding the ion. The MM waters were confined to this sphere using the radial restraint, $E_{quartic} = k_{quartic}{}^2(r - \Delta r_{off})^2[(r - \Delta r_{off})^2 - P_1]$, with $k_{quartic} = 0.2$ kcal$^{0.5}$ Å^{-2}, $P_1 = 2.25$ Å, and $\Delta r_{off} = 14$ Å. For all QM/MM simulations, the QM region contained the ion and the 12 water molecules nearest to it. The QM and MM models, the coupling between them, and the boundary potential to enforce their separation are described in the following sections.

Quantum Model. Although quantum mechanical simulation methods are "first principles" techniques, many approximations must be employed for ab initio molecular dynamics simulations to be computationally practical. To date, simulations of alkali ion solvation have employed relatively inexpensive quantum chemical methods, such Hartree−Fock (HF) theory and Density Functional Theory (DFT). The most significant approximation of the HF model is the complete neglect of instantaneous electron correlation. In comparison, DFT approximates both exchange and correlation through an exchange-correlation functional. Both of these methods can produce significant errors in the calculation of intermolecular interactions.[32] We have used the PBE functional[33] in our QM/MM DFT ion solvation simulations, as it is a robust and efficient pure functional (i.e., exchange integrals are not required) that is relatively accurate in the calculation of intermolecular interactions.[34]

The MP2 model is a second-order perturbative correction to HF theory.[35] This model is significantly more accurate in the calculation of intermolecular interactions than HF theory and performs more reliably than most popular DFT functionals. As it is considerably more computationally expensive than HF and DFT methods, it has not been employed in previous QM/MM

molecular dynamics simulations of ion solvation. By using the high performance parallel computing and the efficient Resolution of Identity (RI) MP2 method,[36] we have performed the first reported MP2-level simulations of Na^+ and K^+ hydration. These simulations serve as a first principles check on the DFT and force field simulations.

The basis set is another feature of AIMD simulations that can affect the accuracy of the results. To date, relatively small double-ζ basis sets have been used to moderate the computational cost of long QM/MM MD ion solvation simulations.[25−27,37] The basis set truncation and basis set superposition errors associated with using these smaller basis sets introduces an additional source of error. Simulations that employ the CPMD code use a planewave basis in combination with a pseudopotential representation of core electrons. Basis set superposition error does not occur with planewave basis sets; however, both the type of pseudopotential and the completeness of the planewave basis can affect the accuracy of the simulations.

In these QM/MM simulations, we have aimed to reduce the error due to basis set truncation as much as possible by using the triple-ζ basis sets, which are considerably more complete than the double-ζ basis sets used in other studies. Case in point, for a system containing one K^+ ion and 12 water molecules, the triple-ζ def2-TZVP basis set used in this study is comprised of 549 basis functions, while the corresponding double-ζ basis set, def2-SVP, is comprised of only 312 basis functions. Test calculations on the solvation structure of K^+ using the def2-SVP basis set confirmed that approximating the QM electron density with this smaller double-ζ basis set results in a different ion solvation structure, with a much wider RDF peak and a coordination number of 8.8 (see the Supporting Information).

The MM Model. The MM component of a QM/MM simulation also requires consideration. The MM water model creates a dynamic electric field around the QM region and has electrostatic and Lennard-Jones attractions and repulsions with the QM atoms, although these effects depend on the MM method that is used. The dielectric constant for bulk liquid water is significantly overestimated by popular water models such as TIP3P (TIP3P, $\varepsilon = 92 \pm 5$; experimental, $\varepsilon = 78$). To avoid this, we have used the recently developed Drude polarizable SWM4-NDP model,[38] which has a bulk liquid dielectric constant that is in close agreement with experimental results (SWM4-NDP: $\varepsilon = 79 \pm 3$). This MM method is expected to produce a more realistic dynamically polarizable electric field around the QM region.

QM/MM Coupling. A key component of QM/MM methods is the coupling between the point charges of the MM region and the electron density of the QM region. In the popular QMCF ion solvation model, this is accomplished by calculating partial atomic charges for the QM region at each time step, then using Coulomb's law to calculate the pairwise electrostatic interaction.[37] It is necessary to assign atomic charges to the QM atoms such that the forces between the MM point charges and the QM electron density are reproduced accurately by classical pairwise point-charge−point-charge interactions. This type of charge fitting procedure is a longstanding challenge in quantum chemistry and is fundamentally inexact. We avoid this approximation by directly calculating the QM/MM electrostatic interactions through the inclusion of one-electron integrals between the MM point charges (q_n) and the basis function pairs (μ, ν) of the QM Fock matrix:[39]

$$F_{\mu\nu}^{\mathrm{QM/MM}} = F_{\mu\nu}^{\mathrm{QM}} - \sum_{n}^{\mathrm{MM}} \left\langle \mu \left| \frac{q_n}{r_n} \right| \nu \right\rangle \tag{1}$$

Separation of the Inner QM Region from the Outer MM Region. Intuitively, the most natural separation of the system into QM and MM regions in QM/MM ion solvation simulations is to treat the ion and a small number of the nearest solvent molecules at the QM level and to represent the surrounding bulk solvent at the MM level. A complication to this procedure occurs when the QM solvent molecules, which are initially near the ion, diffuse away and exchange with the MM solvent molecules from the surrounding bulk liquid. In practice, such a naïve QM/MM simulation would necessarily lead to configurations where some QM molecules are located in the bulk and some MM molecules are located near the ion.

A simple strategy to ensure that the n QM solvent molecules do not move away from the ion is to impose a constraint to keep them within a fixed spherical region around the ion. In a simulation, this procedure has the undesirable effect of introducing an artificial bias into the system by strictly enforcing a constant number n of solvent molecules in the volume around the ion. To remove such a bias, it is necessary to average the results over all possible values of n, weighed by the probability $P(n)$. This approach essentially encounters the same difficulties as QCT due to the problematic evaluation of the probability $P(n)$. Allowing molecules to dynamically exchange between the QM and MM regions avoids the need to compute $P(n)$ explicitly but raises the issue of discontinuities in the potential energy surface. Sophisticated methods have been developed to produce continuous energy and forces by defining a switching function to interpolate between QM and MM forces in a buffer region between the inner sphere and the bulk. The ONIOM-XS of Morokuma and Kerdcharoen[30] and the QMCF method of Rode and co-workers[37] were early examples of this strategy. Later improvements by Truhlar and co-workers[31] and Bulo et al.[40] resolved issues of energy and momentum conservation. The widespread use of these methods has been hindered by the technical difficulty of incorporating them into existing MD codes. Additionally, artifacts can be introduced into the simulation by the use of nonphysical interpolated QM and MM forces in the buffer region. Finally, one drawback is that the total computational cost can become significant due to the obligation of calculating the QM forces on the solvent molecules in the inner and buffer regions.

To avoid the issues associated with existing QM/MM solvent boundary schemes based on a fixed-space inner region, we propose here an alternative method to separate the QM and MM solvent molecules, the Flexible Inner Region Ensemble Separator (FIRES). The formulation of the method starts by considering the configurational integral of an ion in a homogeneous solvent separated into the solute degrees of freedom ($\mathbf{r}_{\mathrm{ion}}$) and the N solvent degrees of freedom:

$$Z = \int \mathrm{d}\mathbf{r}_{\mathrm{ion}} \frac{1}{N!} \int \mathrm{d}\mathbf{r}_1 \int \mathrm{d}\mathbf{r}_2 \ldots \int \mathrm{d}\mathbf{r}_N \, \mathrm{e}^{-U/k_{\mathrm{B}}T} \tag{2}$$

noting that the $N!$ in the denominator is introduced to account for the equivalent configurations arising with N indistinguishable solvent molecules. Alternatively, the configurational integral of the solvent degrees of freedom can be separated into an integral covering the indices of the n solvent molecules

nearest the solute (1, ..., n) and the remaining $N - n$ outer solvent molecules.

$$Z = \int d\mathbf{r}_{ion} \frac{1}{n!} \int d\mathbf{r}_1 \int d\mathbf{r}_2 \ldots \int d\mathbf{r}_n \frac{1}{(N-n)!} \int' d\mathbf{r}_{n+1} \int' d\mathbf{r}_{n+2} \cdots \int' d\mathbf{r}_N \, e^{-U/k_B T} \quad (3)$$

The prime indicates that the integral is performed over the region of space outside the outermost solvent molecule of the set 1, ..., n. Within this rewriting of Z, it is possible to sample a configurational subspace of this system that is equivalent to that in eq 3 by carrying out a simulation where the set of n inner solvent molecules is strictly constrained to remain nearest the solute relative to the remaining $(N - n)$ outer solvent molecules. The (flexible) separation between n inner and $N - n$ outer solvent molecules that is defined by eq 3 is strictly exact. In other words, simulations are expected to yield rigorously correct thermodynamic averages as long as the solvent molecules from the inner and outer regions are not allowed to exchange and swap during the simulation. This analysis previously provided the basis for the statistical mechanical formulation of the mixed explicit−implicit simulation method called Spherical Solvent Boundary Potential (SSBP).[11] In SSBP, the solute is solvated by a number of explicit solvent molecules, while the influence of the surrounding solvent molecules outside this explicit inner sphere is taken into account via a mean-field potential of mean force. Here, we have extended this strategy to carry out mixed QM/MM simulations in which the set of n solvent molecules nearest a solute is treated using at the QM level while the rest of the solvent molecules are accounted for explicitly and treated with an MM force field. This provides a straightforward means to model solvation of an ion where the nearest n solvent molecules are always represented with a QM potential and the outermost solvent molecules are treated with an MM potential without employing a switching function or a strict confinement restraint.

One requirement of this formalism is that we must find a way to sample the ensemble where the same n solvent molecules are always nearest the solute. The idea is to forbid any of the MM solvent molecules from being closer to the ion than any of the QM solvent molecules. In other words, none of the MM molecules must be allowed to enter the sphere of radius R_{inner}, defined as the distance between the solute ion and the inner solvent molecule most distant from it:

$$R_{inner} = \max(r_1, r_2, \ldots r_n) \quad (4)$$

Here, R_{inner} must be determined instantaneously at each time step. This condition is illustrated in Figure 1. In principle, this condition could be imposed by modifying the equations of motion to enforce a spherical constraint on the inner sphere solvent molecules with reflecting collisions. However, with current MD programs it is easier to apply a differentiable potential to implement the condition. In practice, we have found that enforcing the condition can be accomplished easily by imposing a simple half-harmonic restraint that exerts a repulsive radial force on any outer sphere molecules that are closer to the ion than the most distant inner sphere solvent molecule. We refer to this restraining potential as the Flexible Inner Region Ensemble Separator (FIRES):

$$E_{FIRES} = \frac{1}{2} \sum k_{FIRES}(r_j - R_{inner})^2 \quad (5)$$

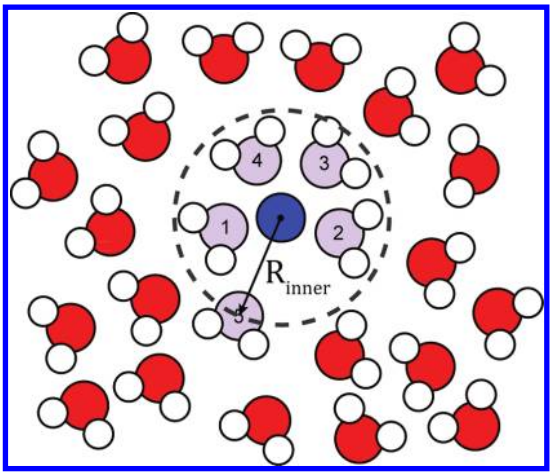

Figure 1. Schematic of the FIRES restraint. Five solvent water molecules (purple) are in the inner sphere around the solute ion (dark blue). All outer region solvent molecules (red) are restrained to remain outside the distance between the solute and the outermost inner sphere molecule (R_{inner}).

Through numerical tests, we found that a force constant k_{FIRES} of 500 kcal Å^{-2} was effective at maintaining this condition without causing numerical instability. As the FIRES restraint imposes counterintuitive nonphysical forces on the system, we have run tests on systems containing only MM models to compare the free and FIRES restrained RDFs to show that this procedure does not introduce any significant artifacts into the simulation results. Our test system was comprised of a 14 Å sphere of 451 SWM4-NDP waters with a K^+ ion at the origin. Molecular dynamics simulations were run for 3 ns for an unrestrained system and a system where a FIRES restraint was imposed to create an inner set of 12 water molecules. The K^+−O RDFs for these simulations are presented in Figure 2. The RDF generated from the system with the FIRES restraint

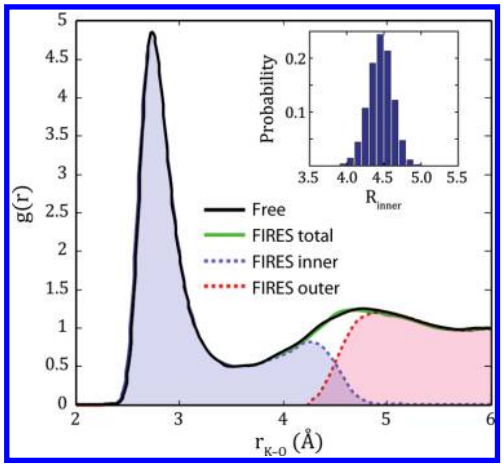

Figure 2. The unrestrained K^+−O RDF of K^+ in the center of a 451 SWM4-NDP water sphere computed from 3 ns MD simulations (black line). The RDF of the simulation where the nearest 12 water molecules were restrained using the FIRES restraint from eq 5 are represented with a green curve. The component from the first inner set of water molecules (n = 1−12) is shown in blue. The component from the rest of the water molecules is shown in red. The inset figure shows a histogram of the R_{inner} radius for the FIRES restraint of this simulation (i.e., the distribution function of the 12th outermost water molecule).

dx.doi.org/10.1021/ct300091w | J. Chem. Theory Comput. 2012, 8, 3526−3535

imposed was effectively identical to the RDF calculated from the unrestrained simulation over the region of interest ($0 < r < 4$ Å), although small deviations are apparent in the region where the FIRES restraint is active for this simulation ($4 < r < 5$ Å). These deviations are much smaller than those that generally result from sampling error in AIMD simulations. This demonstrates that the FIRES restraint does not introduce a large bias for alkali ion solvation simulations. This illustrative test was carried out to demonstrate and illustrate the validity of the formal separation of the configurational integral into an inner and outer region when the sorting potential based on eq 5 is used. Since the validity of the theoretical framework based on eq 3 is strictly independent of the underlying energy surface, the polarizable MM model was used to enable a direct comparison with the radial distribution function obtained from an unbiased simulation (without the FIRES restraint).

The FIRES restraint results in a flexible boundary condition where the radius enclosed by the QM region varies over the course of the trajectory (Figure 2, inset). Including a sufficiently large number of water molecules can ensure that the section of the RDF that is of interest is exclusively enclosed by the QM region. For Na^+ and K^+, including 12 water molecules in the inner region ensures that the region containing the first coordination sphere ($r < 3.5$ Å) is always within the QM region.

The number of molecules that can be included in the inner region is limited by the increased computational cost of the QM calculation and the increasing frequency that the artificial FIRES force must be activated to repel an outer region molecule from the inner region. This could be circumvented by implementing a strict reflective boundary condition instead of the restraining potential given by eq 5. Another obvious limitation is that dynamic properties, such as water exchange rates, cannot be computed when a FIRES restraint is imposed. Interestingly, it might be possible to exchange the momenta of the inner (QM) and outer (MM) solvent molecules during a virtual collision (i.e., when they both attempt to cross R_{inner}) to produce a more realistic time-propagation of the QM/MM system. Nevertheless, this procedure is an effective means for us to compute time-averaged solvation properties for small solutes with high-level QM methods.

Computational Details. All QM/MM simulations were performed using a modified version of CHARMM c36a6 interfaced with TURBOMOLE 6.3.[41] The gukini.src source file, containing the CHARMM/GAMESS and CHARMM/Q-Chem[42,43] interfaces, was modified to support TURBOMOLE as the external quantum chemistry program. The def2-TZVP basis set was used for all atoms.[44] For the elements contained in the systems studied here, this is a triple-ζ all-electron basis set with an additional set of higher-angular momentum basis functions to represent electron polarization. The m5 grid was used for the exchange-correlation integration, and a tolerance 10^{-7} Hartree was used in the SCF iterations to ensure that the DFT gradients were calculated accurately. The Resolution of Identity (RI) approximation was employed for both the DFT and MP2 calculations.[36,45] Benchmark calculations showed that this approximation does not significantly change the coordination energies or structures of ion−water clusters in comparison to conventional DFT and MP2.

The propagation of the molecular dynamics simulations was performed using the VV2 module of CHARMM using a 1 fs time step. The Drude polarizable SWM4-NDP model[38] was used to represent the outer sphere water molecules. The temperature was maintained using a dual-Langevin thermostat. Atomic centers were maintained at 298.15 K with a frictional coefficient of 5 ps^{-1}, while the Drude particles were maintained at 1 K with a frictional coefficient of 10 ps^{-1}. All water molecules were kept rigid using the SHAKE algorithm.[46]

The QM/MM Lennard-Jones interactions were adjusted so that the dimerization energy and hydrogen bonding distance of the water dimer for a QM donor/MM acceptor and QM acceptor/MM donor pair matched the QM−QM minimum energy geometry. These parameters are included in the Supporting Information.

The Drude simulations were equilibrated for 100 ps prior to generating a 1 ns trajectory for analysis. The QM/MM DFT simulations were initiated from the equilibrated Drude simulation and were equilibrated again for 10 ps prior to generating a 50 ps trajectory. The QM/MM MP2 simulations were initiated from the equilibrated QM/MM DFT simulation. As the QM/MM MP2 simulations are far more computationally expensive, these simulations were shortened to 5 ps of equilibration followed by a 14 ps simulation saved for analysis.

The Car−Parrinello molecular dynamics simulations were performed using CPMD version 3.13.2,[47] using the PBE functional with Goedecker-type pseudopotentials.[48] A plane-wave cutoff of 100 Ry was used. The simulations were performed using a cubic simulation cell of length 11.31 Å containing the ion and 48 water molecules. Nosé−Hoover thermostats[49,50] were used to regulate the temperatures of the nuclei and fictitious electronic masses; the nuclei were maintained at temperature of 298.15 K using a thermostat frequency of 2500 cm^{-1}, while the electronic degrees of freedom were maintained at 0.02 K using a thermostat frequency of 10 000 cm^{-1}.[49] The fictitious electronic mass was 600 amu. A time step of 0.097 fs (4 au) was used. The CPMD systems were equilibrated for 10 ps prior to the generation of 50 ps trajectories.

RESULTS

The Flexible Inner Region Ensemble Separator (FIRES) is a rigorous method to maintain the integrity of the QM and MM set of molecules in the inner and outer regions, respectively. For the sake of clarity, it is worth briefly contrasting FIRES with the perhaps more familiar construct of quasi-chemical theory (QCT). Formally, QCT starts by defining a fixed spatial inner region (or observation subvolume) around the solute and then works out the probabilities for finding n solvent molecules occupying this region.[55] The ensuing expressions are rigorous and exact, as long as the number of solvent molecule in the inner region is allowed to fluctuate, showing that QCT is formally equivalent with the small volume grand-canonical ensemble (SSGCE).[55] In contrast, the flexible separation expressed by eq 3 works by resorting the labels of indistinguishable solvent molecules in the fluid.[11] The spatial separation between the n inner solvent molecules and the $N - n$ outer ones is flexible in space but fixed with respect to the labels. This construct yields average properties that are strictly consistent with equilibrium statistical mechanics.[11]

Na^+ Solvation. The established view of Na^+ hydration is of a fairly narrow first coordination sphere containing five or six water molecules. In terms of the RDF, the first peak is sharp and narrow and is followed by a near-zero first minimum. All of the methods we have evaluated here are generally consistent with this, although there are significant distinctions between them. The RDFs calculated using the four methods are

presented in Figure 3. Each of these methods predicts the maximum of $g(r_{max})$ to be located between 2.3 and 2.5 Å and a

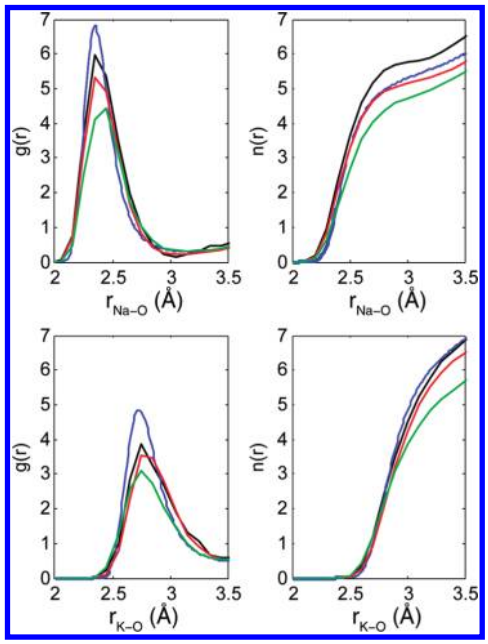

Figure 3. Calculated RDFs (left) and number distrubtions (right) of Na^+ (top) and K^+ (bottom). A bin width of 0.01 Å was used for the Drude model, while 0.1 Å bins were used for the shorter ab initio simulations. Coloring as follows: QM/MM MP2, black; Drude, blue; QM/MM DFT, red; CPMD, green. All of the RDFs are given in the Supporting Information.

$g(r)$ that is effectively zero at $r < 2.0$ Å. These values are in good agreement with neutron diffraction data, which gives an average nearest-neighbor Na−O distance of 2.40 ± 0.05 Å,[8] and with recent large-angle X-ray scattering (LAXS) data, which gives an average Na−O distance of 2.43 ± 0.02 Å.[51] The width of the peak is also generally consistent, and each method shows a deep minimum between 3.0 Å and 3.5 Å. The height of the first peak is more variable; the CPMD simulation predicts a $g(r_{max})$ of 4.4, while the DFT and MP2 QM/MM simulations predict significantly higher peaks at 5.3 and 6.0, respectively. The $g(r_{max})$ of the Drude model RDF has the highest peak, at 6.8.

These trends are even more evident in the $n(r)$ distribution (Figure 3). Although the RDF peak is shorter, the QM/MM MP2 model has a slightly broader first peak, so the $n(r)$ rises more sharply and then plateaus at $n = 6$. At $r = 3.2$ Å, $n(r)$'s for the MP2 and Drude models are close (5.6 and 5.8, respectively), with the QM/MM DFT model predicting a lower coordination number (5.4), with the CPMD simulation predicting the lowest coordination number (5.1). Both the Drude and MP2 models predict that the most probable Na^+ coordination numbers is 6, with significant probabilities for a coordination number of 5, while 5 becomes the most probable coordination number for the QM/MM DFT and CPMD models (see the Supporting Information for coordination number probability distributions). The coordination numbers predicted by these models are summarized in Table 1.

The structural differences of these simulations can also be characterized by examining the tilt and angular distributions of the first coordination shells. The tilt distribution shows alignment of the principal axis with the first solvation sphere

Table 1. Coordination Number ($n(R_i)$) for the First Coordination Sphere ($R_{Na-O} < 3.2$ Å, $R_{K-O} < 3.5$ Å)

	n_c	
method	Na^+	K^+
QM/MM MP2	5.8	7.0
Drude	5.6	7.0
QM/MM DFT	5.4	6.8
CPMD	5.1	5.8

of water molecules with respect to the ion. The tilt distributions calculated using the four methods are presented in Figure 4. An

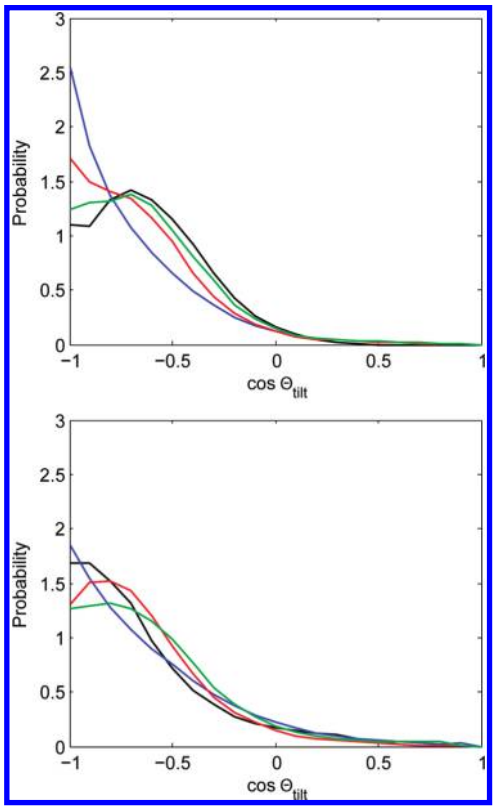

Figure 4. Tilt angle distributions (ion−O−H bisector) for the first coordination sphere of Na^+ (upper panel) and K^+ (lower panel). Cutoffs were defined as $R_{Na-O} < 3.2$ Å and $R_{K-O} < 3.5$ Å. Coloring as follows: QM/MM MP2, black; Drude, blue; QM/MM DFT, red; CPMD, green.

angle of $\cos\theta = -1$ ($\theta = 180°$) corresponds to the alignment of the dipole vector of a coordinating water molecule with the ion. For Na^+, the Drude model shows a sharp cusp at $\cos\theta = -1$, while the QM models have a flatter probability distribution between $-1 < \cos\theta < -0.75$ ($180° > \theta > 139°$). This trend was previously noted in a CPMD simulation by White et al.[20] As the Drude Na^+-OH_2 potential energy surface is in excellent agreement with the ab initio models over this interval (see the Supporting Information), this is likely an effect of interligand interactions. The waters within the QM models have more flexibility in their electronic polarization than the Drude particles of SWM4-NDP molecules, so these broader distributions may simply reflect the better ability of the QM models to provide stable charge distributions over a broader range of tilt orientations between 0 and 45°.

dx.doi.org/10.1021/ct300091w | J. Chem. Theory Comput. 2012, 8, 3526−3535

The angular distribution function (ADF) gives the distribution of angles formed between the ion and two inner-sphere water molecules. The ADFs for the four methods evaluated here are presented in Figure 5. The ADF shows a

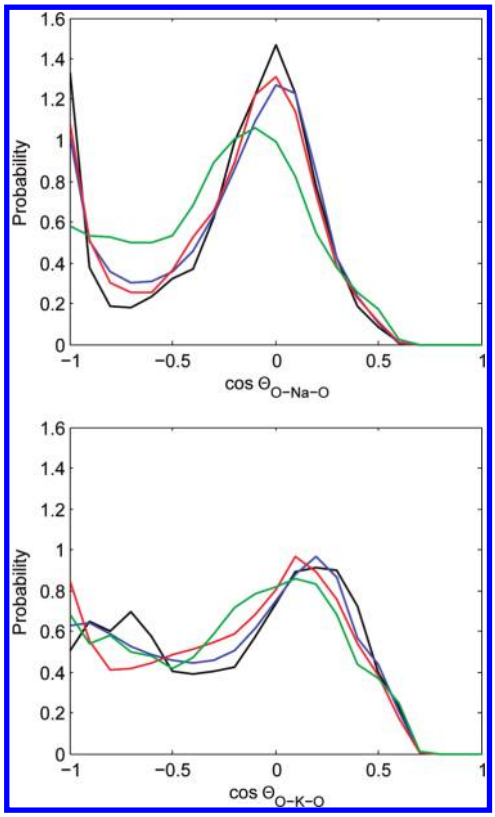

Figure 5. Water−ion−water angle distributions for first coordination spheres of Na^+ and K^+ (R_{Na-O} < 3.2 Å, R_{K-O} < 3.5 Å). Coloring as follows: QM/MM MP2, black; Drude, blue; QM/MM DFT, red; CPMD, green.

significant distinction between CPMD and the other models. The ADFs of the Drude, QM/MM DFT, and QM/MM MP2 show maxima at cos $\theta = -1.0$ ($\theta = 180°$) and cos $\theta = 0.0$ ($\theta = 90°$), consistent with a high probability of 6-fold coordination in octahedral-like structures. The CPMD simulation has a broad, flat distribution with a maximum at cos $\theta = -0.1$ ($\theta = 95°$), consistent with a broader range of angles that can occur when the coordination number is 5.

K^+ Solvation. K^+ is generally considered to be the first alkali ion that has significant diffusive hydration character, although various studies have reached differing conclusions about the degree of this character. All of the methods evaluated here are consistent with the trend of the first peak of the RDF being shorter but broader than that of the Na^+−O RDF and the first minimum being higher (Figure 3). The maximum of the RDF occurs at a similar radius for all of the methods, occurring at 2.75 Å for the Drude, QM/MM MP2, and CPMD simulations. This is in good agreement with the average nearest-neighbor K−O distance of 2.73 ± 0.05 Å determined by EXAFS[7] and the K−O distance of 2.81 ± 0.01 Å determined by LAXS[51] but is slightly higher than the r_{max} = 2.65 Å determined on the basis of neutron diffraction.[6] In each case, $g(r)$ is effectively zero below 2.4 Å. As in the Na^+ simulation, the maximum of the CPMD RDF is the lowest, with a $g(r_{max})$ of 3.14. The $g(r_{max})$ of QM/MM DFT is significantly higher, at 3.49. The Drude and MP2 models have even higher maxima: at 4.85 and 4.16, respectively, which is in the same range as the value determined on the basis of neutron diffraction ($g(r_{max})$ = 4.5). These repeat the trend observed for Na^+, although QM/MM DFT lies further from the Drude and MP2 results for K^+.

In terms of the $n(r)$, the Drude, QM/MM DFT, and QM/MM MP2 models are in good agreement, rising rapidly above r = 2.5 Å and reaching 7 at r = 3.5 Å (Figure 3). The CPMD model is a distinct outlier again, only reaching 5.7 at r = 3.5 Å. As the $g(r)$ never reaches 0 for any of these methods (in fact, it remains between 0.5 and 0.7 through the range considered the first minimum), $n(r)$ is always increasing and does not plateau. This is consistent with K^+ having a broad and diffuse first coordination shell. The consensus of the models other than CPMD is that K^+ has a coordination number near 7. Significantly, a K^+ coordination number of 7 was also observed for the AMOEBA force field, although the form and parametrization of this model differs considerably.[52]

The tilt distributions of K^+, presented in Figure 4, are generally in good agreement across all methods, although the MP2 and Drude models have distributions that are more peaked at cos $\theta = -1$ (180°). Significantly, for the ab initio methods, the distributions are similar to those for Na^+, suggesting that Na^+ and K^+ actually have comparable orientational effects on coordinating water molecules. As for Na^+, the Drude model gives sharper K^+−OH_2 tilt angle distributions than the QM models, although this effect is much smaller for K^+. This suggests that this overorientation of waters in the Drude model is most significant for small ions.

The ADFs of the QM/MM MP2, Drude, and QM/MM DFT models, presented in Figure 5, are generally very similar; the ADF is reasonably flat between cos $\theta = -1$ and cos $\theta = -0.25$, followed by a broad peak that reaches a maximum between cos θ = 0.1 and cos θ = 0.2 that goes to zero when cos $\theta > 0.7$ ($\theta < 46°$). Although the distribution from CPMD is similar, the peak is broader, beginning at cos $\theta = -0.5$ ($\theta = 120°$), consistent with a less ordered structure containing lower coordination numbers.

Basis Set Superposition Error. A persistent challenge in QM/MM simulations with atom-centered basis sets is the effect of Basis Set Superposition Error (BSSE), where the basis set incompleteness at an atomic center results in a spurious additional intermolecular interaction energy. In other words, the basis set representation changes when the nuclei change their positions, a situation that is not present in calculations carried out with plane-wave basis sets. This issue led us to use a more complete triple-ζ basis set to minimize BSSE. To quantify the magnitude of BSSE still present in our simulations, we selected 50 frames from each of the QM/MM MP2 trajectories and calculated its BSSE energy using a counterpoise correction, where each QM water molecule and the ion were defined as separate fragments. Although the BSSE was still sizable, with these frames having an average BSSE energy of 7% of the total interaction energy, the BSSE energy was similar for each of these frames, with a BSSE standard deviation of 0.1 kcal mol^{-1} over the frames considered. The addition of such an energy correction, E_{BSSE}, would perturb the average of any property A, in the following way:

$$\langle A \rangle = \frac{\langle A\ e^{-E_{BSSE}/k_B T} \rangle_0}{\langle e^{-E_{BSSE}/k_B T} \rangle_0} \quad (6)$$

dx.doi.org/10.1021/ct300091w | J. Chem. Theory Comput. 2012, 8, 3526−3535

where $\langle ... \rangle_0$ represents an ensemble average with the unperturbed Hamiltonian.

The constancy of the BSSE energy suggests that for this system, this amount of BSSE is present regardless of the configuration, serving as a constant offset in energy rather than causing a large systematic bias toward certain configurations. Critically, the average BSSE of configurations for coordination numbers $n = 5$ and $n = 6$ for Na^+ and $n = 6$ and $n = 7$ for K^+ differed by less than 0.1 kcal mol^{-1} in each case, so the presence of BSSE in our simulations would not be expected to cause a systematic shift in the calculated coordination number distributions. It should also be noted that the Boys counterpoise correction used to estimate the BSSE has the tendency to overestimate the magnitude of this error. Nevertheless, when the computational resources become available, repeating these simulations using a quadruple-ζ basis set would allow us to achieve greater accuracy by further reducing error due to basis set incompleteness and basis set superposition.

DISCUSSION

A novel and rigorous scheme to partition a system corresponding to an ion in the liquid phase into an inner QM region and an outer MM region must first and foremost yield correct probabilities for the various configurations of the system. If the partition is based on fixed spatial criteria, then it is necessary to either evaluate the probability $P(n)$ to have n solvent molecules within the inner region as in QCT, or to allow the solvent molecules to smoothly switch their representation as they enter and exit the QM inner region. An alternative and formally valid procedure implemented in FIRES consists of constructing the partition scheme from an ordering criterion by preventing the exchange and mixing of QM and MM molecules. In this case, there is no fixed spatial separation between QM and MM regions; the virtual boundary region is flexible and dynamical.

The trends across the present simulations allow us to make a few limited conclusions about the performance of these methods for modeling alkali ion hydration. In general, the Drude simulations give sharper RDF peaks than the ab initio methods. This is consistent with the overly steep repulsive wall of the Lennard-Jones potential of the M−O interaction, which is particularly significant for ionic systems where the electrostatic interaction term pulls the two atoms into distances where the Lennard-Jones term is strongly repulsive. The ab initio methods produce a first RDF peak that is not as steep as those produced from the Drude simulation, which reflects the first-principles treatment of the Pauli repulsion between the ion and oxygen atoms, giving a slightly more gradual repulsive wall in comparison to the Lennard-Jones r^{-12} repulsive term.

The systematically different results of the CPMD simulations are also notable. The CPMD simulations consistently predicted smaller RDF peaks and lower coordination numbers compared to the other methods. The QM/MM DFT and CPMD simulations we report employ the same exchange-correlation functional (PBE), although they produced significantly different ion solvation structures for both Na^+ and K^+. This suggests that the deviation between the two methods does not reflect an inherent failure of DFT to describe ion−water interactions. Truncation error of the CPMD planewave basis set or the atomic core pseudopotentials and the tendency of this type of simulation to predict an overly ordered bulk water structure[53,54] are other possible sources of deviation. It should be noted that the CPMD simulations performed here differ from the QM/MM simulations because they are performed under periodic boundary conditions and the water geometry was not rigidly constrained, although neither of these differences is expected to have a large effect on the local hydration structure of these relatively large monovalent cations.

The most chemically significant difference between the hydration structures determined in CPMD simulations in comparison to the other molecular dynamics simulations is that the coordination numbers were lower than those from the Drude and MP2 simulations by approximately 1. The CPMD simulations give coordination numbers of 5.1 and 5.8 for Na^+ and K^+. This trend is similar to those reported in other CPMD studies. This result is consistent with the RDFs, where the first peak of the CPMD simulation occurs at the same position but is of a smaller magnitude.

The coordination numbers determined using the MP2 model are in sharp contrast to the coordination numbers determined using a primitive version of QCT (pQCT), which predicted that a coordination number of 4 should be optimal for both ions.[21,22] One source of this difference could be that we used an MP2/triple-ζ QM region and a SWM4-NDP MM region. In pQCT studies, the inner region has typically been treated at the DFT level (e.g., B3LYP/6-31+G(d,p)), while the surrounding outer bulk region was represented as a macroscopic continuum dielectric. An additional, and possibly larger source of error, may have been the use of the rigid rotor harmonic oscillator (RRHO) partition function to approximate the configurational integrals involving the ion and the n water molecules in pQCT.[55]

The tendency of the PBE DFT functional to overestimate water−water repulsion due to neglect of the dispersive attraction is one possible explanation of the discrepancy between the DFT and MP2 simulations. In principle, this problem could be resolved by a dispersion correction. We tested the dispersion correction of Grimme et al.[56] for the K^+ QM/MM model and found the coordination number was increased to 7.8 (without this correction, the coordination number is 6.8); however, the peak was also significantly broadened, and the minimum of the RDF was effectively eliminated (see the Supporting Information). We observed a similar trend in a previously reported dispersion-corrected CPMD simulation of K^+ hydration.[1] As this result is inconsistent with experimental data and the other simulations, we conclude that a simple dispersion correction is not sufficient to make PBE DFT based ion solvation simulations quantitatively accurate.

As the MP2 method is the most reliable ab initio method employed here, this is the best method to evaluate the accuracy of all other models. Despite the relatively short length (14 ps) of the MP2 simulations, these simulations provide the most reliable results about the hydration structure of Na^+ and K^+. Although the $g(r_{max})$ and coordination numbers from the Drude simulation are slightly above those from the MP2 simulation, the MP2 and Drude force field results are in generally good agreement. In contrast, the CPMD simulations systematically predict less sharp peaks and lower coordination numbers. The O−ion−O angular distributions also show that the CPMD simulation predicts a substantially different ion solvation structure than the other methods. The accuracy of the Drude model is also supported by good agreement with experimental ion hydration enthalpies, solvation free energies, and self-diffusion coefficients of alkali salts in water.[57]

In principle, alkali cation hydration is a simple phenomenon. Even approximate dielectric descriptions, as simple as the Born model, can account for the large hydration free energies with near-quantitative accuracy.[58] Nevertheless, more detailed atomistic descriptions are needed to understand complex biochemical systems. Yet, almost any detailed model will be sensitive to the computational methodology used. As all of the methods are generally in good agreement for the position of r_{max}, it seems unlikely that the ion−water interactions alone are the cause of these differences. The solvation structure of ions also requires a realistic description of water−water interactions in the bulk environment, and of the atypical arrangements that occur around ions. CPMD simulations of water with contemporary DFT functionals have been determined to be significantly overstructured,[53] so accurate calculation of these interactions ab initio requires more computationally expensive models (i.e., post Hartree−Fock ab initio models or improved DFT functionals[59,60]). In this respect, force fields have an advantage, as they can be parametrized to optimally reproduce the experimental properties of water using a greatly simplified potential.

Although more extensive simulations and experiments would be needed to be more conclusive, it appears that the Drude polarizable model performs remarkably well even in comparison to expensive QM/MM MP2 calculations. Nevertheless, there is an evident trend for the Drude model to predict sharper RDF peaks and higher coordination numbers. Also, the tilt distributions of Na^+ suggest that the Drude model is overestimating the tendency of the water molecule to align its dipole with the ion. It is however worth noting that such deviations do not arise from an intrinsic inaccuracy of the ion−water monohydrate energy surface (see the Supporting Information), indicating that they must reflect some complex features of the water−water interactions. As the Drude force field parameters for these ions were optimized to reproduce experimental hydration energies, it is unlikely that these deviations might be resolved by reparameterizing the present force field potential. A more elaborate force field with a more realistic repulsive potential,[61] polarization anisotropy,[62] or Thole screening[57] could avoid some of these discrepancies. Notwithstanding these differences, the existing Drude force field is remarkably successful at reproducing the same distributions as the QM/MM MP2 simulations at a roughly 20000-fold smaller computational cost.

CONCLUSION

We have performed molecular dynamics simulations of the solvation of Na^+ and K^+ in water using the Drude polarizable force field, a QM/MM DFT model, a QM/MM MP2 model, and a CPMD model. We employed large triple-ζ basis sets in our QM/MM simulations to minimize error due to basis set truncation and superposition. The QM/MM models employed the SWM4-NDP polarizable water model for the outer sphere waters and the novel FIRES boundary potential to enforce the condition that the water molecules nearest the ion were represented with QM. The DFT QM/MM and CPMD simulations tended to predict less steep peaks in the RDF and smaller coordination numbers than the MP2 QM/MM and Drude models. As the Drude model has been demonstrated to provide good agreement with experimental ion hydration properties and MP2 is generally more reliable than DFT for the calculation of intermolecular interactions, we believe that these models are providing the most realistic description of ion solvation, predicting a coordination number within the range of 5.6−5.8 for Na^+ and 6.9−7.0 for K^+. It is our hope that these accurate results for Na^+ and K^+ will serve as reliable target values in the development of improved force field models, and we have included tabulations of all of the RDFs in the Supporting Information for this purpose.

ASSOCIATED CONTENT

Supporting Information

QM/MM DFT RDF calculated with a dispersion correction, QM/MM DFT RDF calculated with a double-ζ basis set, Na^+−OH_2 and K^+−OH_2 PES, coordination number distributions, partial radial distributions, QM/MM Lennard-Jones parameters, tabulated RDFs. This material is available free of charge via the Internet at http://pubs.acs.org.

AUTHOR INFORMATION

Corresponding Author

*Phone: 773-834-3557. E-mail: roux@uchicago.edu.

Notes

The authors declare no competing financial interest.

ACKNOWLEDGMENTS

This work was supported by the National Science Foundation through grant MCB-0920261. C.N.R. acknowledges NSERC of Canada for a postdoctoral fellowship. These simulations were performed using computational resources at the LCRC Argonne National Lab and the Extreme Science and Engineering Discovery Environment (XSEDE) supported by National Science Foundation grant number OCI-1053575. We thank Professor Hagang Lu for providing CPMD pseudopotentials and input files for K^+. We thank Professor Sergei Noskov and Bogdan Lev for helpful discussions.

REFERENCES

(1) Roux, B.; Bernèche, S.; Egwolf, B.; Lev, B.; Noskov, S. Y.; Rowley, C. N.; Yu, H. *J. Gen. Physiol.* **2011**, *137*, 415−426.
(2) Chandler, D. *Introduction to Modern Statistical Mechanics*; Oxford University Press: New York, 1987.
(3) Neilson, G. W.; Mason, P. E.; Ramos, S.; Sullivan, D. *Phil. Trans. R. Soc. London, Ser. A* **2001**, *359*, 1575−1591.
(4) Ansell, S.; Barnes, A. C.; Mason, P. E.; Neilson, G. W.; Ramos, S. *Biophys. Chem.* **2006**, *124*, 171−179.
(5) Neilson, G. W.; Skipper, N. *Chem. Phys. Lett.* **1985**, *114*, 35−38.
(6) Soper, A. K.; Weckström, K. *Biophys. Chem.* **2006**, *124*, 180−191.
(7) Glezakou, V.-A.; Chen, Y.; Fulton, J.; Schenter, G.; Dang, L. *Theor. Chem. Acc.* **2006**, *115*, 86−99.
(8) Skipper, N. T.; Neilson, G. W. *J. Phys.: Condens. Matter* **1989**, *1*, 4141.
(9) Aaqvist, J. *J. Phys. Chem.* **1990**, *94*, 8021−8024.
(10) Berendsen, H. J. C.; Postma, J. P. M.; van Gunsteren, W. F.; Hermans, J. In *Intermolecular Forces*; Pullman, B., Ed.; Reidel: Dordrecht, The Netherlands, 1981; pp 331−342.
(11) Beglov, D.; Roux, B. *J. Chem. Phys.* **1994**, *100*, 9050.
(12) Joung, I. S.; Cheatham, T. E. *J. Phys. Chem. B* **2009**, *113*, 13279−13290.
(13) Jorgensen, W. L.; Chandrasekhar, J.; Madura, J. D.; Impey, R. W.; Klein, M. L. *J. Chem. Phys.* **1983**, *79*, 926−935.
(14) Lybrand, T. P.; Kollman, P. A. *J. Chem. Phys.* **1985**, *83*, 2923−2933.
(15) Dang, L. X.; Rice, J. E.; Caldwell, J.; Kollman, P. A. *J. Am. Chem. Soc.* **1991**, *113*, 2481−2486.
(16) Whitfield, T. W.; Varma, S.; Harder, E.; Lamoureux, G.; Rempe, S. B.; Roux, B. *J. Chem. Theory Comput.* **2007**, *3*, 2068−2082.
(17) Marcus, Y. *J. Chem. Soc., Faraday Trans.* **1987**, *83*, 2985−2992.

(18) Schurhammer, R.; Engler, E.; Wipff, G. *J. Phys. Chem. B* **2001**, *105*, 10700−10708.
(19) Ramaniah, L.; Bernasconi, M.; Parrinello, M. *J. Chem. Phys.* **1999**, *111*, 1587.
(20) White, J.; Schwegler, E.; Galli, G.; Gygi, F. *J. Chem. Phys.* **2000**, *113*, 4668.
(21) Rempe, S.; Pratt, L. *Fluid Phase Equilib.* **2001**, *183*, 121−132.
(22) Rempe, S.; Asthagiri, D.; Pratt, L. *Phys. Chem. Chem. Phys.* **2004**, *6*, 1966−1969.
(23) Liu, Y.; Lu, H.; Wu, Y.; Hu, T.; Li, Q. *J. Chem. Phys.* **2010**, *132*, 124503.
(24) Leung, K.; Rempe, S. B.; von Lilienfeld, O. A. *J. Chem. Phys.* **2009**, *130*, 204507−11.
(25) Tongraar, A.; Liedl, K. R.; Rode, B. M. *J. Phys. Chem. A* **1998**, *102*, 10340−10347.
(26) Azam, S. S.; Hofer, T. S.; Randolf, B. R.; Rode, B. M. *J. Phys. Chem. A* **2009**, *113*, 1827−1834.
(27) Azam, S. S.; Zaheer-ul-Haq, M.; Qaiser Fatmi, M. *J. Mol. Liq.* **2010**, *153*, 95−100.
(28) Pratt, L.; Beck, T.; Paulaitis, M. *The Potential Distribution Theorem and Models of Molecular Solutions*; Cambridge University Press: Cambridge, U. K., 2006.
(29) Rogers, D. M.; Beck, T. L. *J. Chem. Phys.* **2008**, *129*, 134505−15.
(30) Kerdcharoen, T.; Morokuma, K. *Chem. Phys. Lett.* **2002**, *355*, 257−262.
(31) Heyden, A.; Lin, H.; Truhlar, D. G. *J. Phys. Chem. B* **2007**, *111*, 2231−2241.
(32) Reinhardt, P.; Piquemal, J. P. *Int. J. Quantum Chem.* **2009**, *109*, 3259−3267.
(33) Perdew, J. P.; Burke, K.; Ernzerhof, M. *Phys. Rev. Lett.* **1997**, *78*, 1396−1396.
(34) Zhao, Y.; Truhlar, D. G. *J. Chem. Theory Comput.* **2006**, *3*, 289−300.
(35) Møller, C.; Plesset, M. S. *Phys. Rev.* **1934**, *46*, 618−622.
(36) Weigend, F.; Häser, M. *Theor. Chem. Acc.* **1997**, *97*, 331−340.
(37) Rode, B.; Hofer, T.; Randolf, B.; Schwenk, C.; Xenides, D.; Vchirawongkwin, V. *Theor. Chem. Acc.* **2006**, *115*, 77−85.
(38) Lamoureux, G.; Harder, E.; Vorobyov, I. V.; Roux, B.; MacKerell, A. D. *Chem. Phys. Lett.* **2006**, *418*, 245−249.
(39) Cramer, C. *Essentials of Computational Chemistry: Theories and Models*, 2nd ed.; Wiley: Hoboken, NJ, 2004.
(40) Bulo, R. E.; Ensing, B.; Sikkema, J.; Visscher, L. *J. Chem. Theory Comput.* **2009**, *5*, 2212−2221.
(41) *TURBOMOLE*, V6.3; University of Karlsruhe and Forschungszentrum Karlsruhe GmbH; TURBOMOLE GmbH: Karlsruhe, Germany, 2011. Available from http://www.turbomole.com (accessed March 25, 2012).
(42) Das, D.; Eurenius, K. P.; Billings, E. M.; Sherwood, P.; Chatfield, D. C.; Hodoscek, M.; Brooks, B. R. *J. Chem. Phys.* **2002**, *117*, 10534−10547.
(43) Woodcock, H. L.; Hodošček, M.; Gilbert, A. T. B.; Gill, P. M. W.; Schaefer, H. F.; Brooks, B. R. *J. Comput. Chem.* **2007**, *28*, 1485−1502.
(44) Weigend, F.; Ahlrichs, R. *Phys. Chem. Chem. Phys.* **2005**, *7*, 3297−3305.
(45) Kendall, R. A.; Früchtl, H. A. *Theor. Chem. Acc.* **1997**, *97*, 158−163.
(46) Ryckaert, J.-P.; Ciccotti, G.; Berendsen, H. J. C. *J. Comput. Phys.* **1977**, *23*, 327−341.
(47) *CPMD*, 3.13.2 ed.; IBM Corp. and Max Planck Institute: Stuttgart, Germany.
(48) Goedecker, S.; Teter, M.; Hutter, J. *Phys. Rev. B* **1996**, *54*, 1703−1710.
(49) Nosé, S. *J. Chem. Phys.* **1984**, *81*, 511.
(50) Hoover, W. G. *Phys. Rev. A* **1985**, *31*, 1695−1697.
(51) Mähler, J.; Persson, I. *Inorg. Chem.* **2012**, *51*, 425−438.
(52) Grossfield, A.; Ren, P.; Ponder, J. W. *J. Am. Chem. Soc.* **2003**, *125*, 15671−15682.
(53) Kuo, I. F. W.; Mundy, C. J.; McGrath, M. J.; Siepmann, J. I.; VandeVondele, J.; Sprik, M.; Hutter, J.; Chen, B.; Klein, M. L.; Mohamed, F.; Krack, M.; Parrinello, M. *J. Phys. Chem. B* **2004**, *108*, 12990−12998.
(54) Yoo, S.; Zeng, X. C.; Xantheas, S. S. *J. Chem. Phys.* **2009**, *130*, 221102−4.
(55) Roux, B.; Yu, H. *J. Chem. Phys.* **2010**, *132*, 234101−13.
(56) Grimme, S.; Antony, J.; Ehrlich, S.; Krieg, H. *J. Chem. Phys.* **2010**, 132,.
(57) Yu, H.; Whitfield, T. W.; Harder, E.; Lamoureux, G.; Vorobyov, I.; Anisimov, V. M.; Mackerell, A. D.; Roux, B. *J. Chem. Theory Comput.* **2010**, *6*, 774−786.
(58) Born, M. *Z. Phys* **1920**, *1*, 45−48.
(59) Zhao, Y.; Truhlar, D. G. *Acc. Chem. Res.* **2008**, *41*, 157−167.
(60) Perdew, J. P.; Ruzsinszky, A.; Constantin, L. A.; Sun, J.; Csonka, G. b. I. *J. Chem. Theory Comput.* **2009**, *5*, 902−908.
(61) Buckingham, R. A. *Proc. R. Soc. London, Ser. A* **1938**, *168*, 264−283.
(62) Harder, E.; Anisimov, V. M.; Vorobyov, I. V.; Lopes, P. E. M.; Noskov, S. Y.; MacKerell, A. D.; Roux, B. *J. Chem. Theory Comput.* **2006**, *2*, 1587−1597.